Temporally feathered intensity modulated radiation therapy: a planning technique to reduce normal tissue toxicity

Juan Carlos López Alfonso[a], Shireen Parsai[b], Nikhil Joshi[b], Andrew Godley[b], Chirag Shah[b], Shlomo A. Koyfman[b], Jimmy J. Caudell[c], Clifton D. Fuller[d], Heiko Enderling[c,e], and Jacob G. Scott[b,f,*]

(a) Department of Systems Immunology and Braunschweig Integrated Centre of Systems Biology, Helmholtz Centre for Infection Research, Braunschweig, Germany.
(b) Department of Radiation Oncology, Cleveland Clinic, Cleveland, OH, USA.
(c) Department of Radiation Oncology, Moffitt Cancer Center, Tampa, FL, USA.
(d) Department of Radiation Oncology, MD Anderson Cancer Center, Houston, TX, USA.
(e) Department of Integrated Mathematical Oncology, Moffitt Cancer Center and Research Institute, Tampa, FL, USA.
(f) Department of Translational Hematology and Oncology Research, Cleveland Clinic, Cleveland, OH, USA.

Corresponding Author (∗): scottj10@ccf.org
The authors declare no conflict of interest.

Abstract

Purpose: Radiation-induced normal tissue damage remains a dose-limiting factor in the treatment of cancer with radiation therapy. The purpose of this study is to introduce a novel strategy of radiation therapy planning using canonical radiobiological principles, leveraging time to decrease normal tissue complication probability (NTCP). This strategy is termed temporally feathered radiation therapy (TFRT), in which the fractional dose delivered to each organ at risk (OAR) is varied allowing increased time for normal tissue recovery.
Methods: TFRT plans are generated by altering the fractional dose delivered to the OARs to provide a higher dose once weekly followed by four lower fractional doses. Normal tissue toxicity was compared between TFRT and conventional fractionated radiation plans by using a combination of the Linear-Quadratic (LQ) model to describe the immediate radiation response of normal tissue, and a dynamical model to describe normal tissue repair over time. We simulated various TFRT plans, through which the fractional dose delivered to OARs by standard plans is altered to reduce radiation-induced toxicity. The potential clinical benefit of TFRT was evaluated using the concept of *overall success potential (OSP)*, obtained as the ratio of temporally feathered plans resulting in less NTCP than the corresponding standard treatment plans.
Results: Application of TFRT has potential to reduce normal tissue toxicity with respect to conventionally fractionated radiation therapy. The proposed NTCP model evidenced a window of opportunity to decrease normal tissue toxicity by temporally feathering OARs. The sequencing of high and low fractional doses delivered to OARs by TFRT plans allow increased recovery despite higher total doses to OARs compared to standard treatment plans. The magnitude of toxicity reduction by TFRT planning is dependent on the corresponding fractional dose and organ-specific recovery rate of sublethal radiation-induced damage. For any given OAR recovery rate, a certain range of fractional doses of standard plans exists at which TFRT is able to reduce normal tissue toxicity.
Conclusions: TFRT represents a novel technique for planning and optimization of therapeutic radiotherapy. Application of TFRT to carefully selected clinical cases has the potential to reduce normal tissue toxicity. With widening of the therapeutic ratio, isotoxic radiation therapy plans can be delivered in an effort to allow dose escalation to the planning target. This analysis warrants further study in derivation of patient-specific TFRT plans, as well as clinical evaluation of safety and efficacy.

Keywords: temporally feathered radiation therapy; dosimetry planning; normal tissue complication probability; normal tissue toxicity reduction; therapeutic ratio.

Introduction

With the growing understanding of radiation planning, delivery and effects, its use continues to increase. Currently, it is estimated that about half of cancer patients benefit from curative or palliative radiation therapy at some point during the course of their disease[1]. Historically, the delivery of therapeutic radiation has been limited by the ratio of tumor control probability (TCP) to normal tissue complication probability (NTCP), termed the therapeutic ratio[2]. In this study, we propose a novel technique to further widen the

therapeutic ratio to deliver safer and more effective radiotherapy. Previous research efforts have been directed at maximizing tumor control and minimizing damage to nearby normal tissue by way of improving physical dose distributions, utilizing pharmaceuticals which modulate radiation effect, and optimizing radiation dose and fractionation schemes[3]. Physical dose distribution has been improved with the evolution from 2D to 3D conformal planning and now intensity modulated radiation therapy (IMRT)[4-6]. Preferential tumor kill has been attempted with radiosensitizers and optimizing oxygen distribution[7] and normal tissue sparing has been explored using radioprotectants[8,9]. These are not in routine clinical use and carry the risk of side effects. Several dose and fractionation schemes, which offer benefit to tumor control in specific clinical scenarios, have been widely studied. These include conventional fractionation, hyperfractionation, accelerated hyperfractionation, hypofractionation, and stereotactic body radiation therapy/stereotactic radiosurgery[10-12]. Additionally, current treatment planning techniques allow for heterogeneity and dose escalation even across a tumor while minimizing dose delivered to nearby organs at risk[13]. The efficacy of fractionation schedules has been optimized according to the tumor's inherent radiosensitivity, and more recently, genomic methods have been also postulated[14]. In current practice, fractionated radiation therapy with 1.8 to 2.0 Gy per fraction, remains standard for the majority of cases in the clinical routine.

Through these advancements in radiation oncology, the four pillars of radiobiology have remained the foundation to our understanding of radiation effect on tissue: *(i)* repair of sublethal damage, *(ii)* reassortment of cells within the cell cycle, *(iii)* repopulation, and *(iv)* reoxygenation. Acute normal tissue toxicity is primarily mitigated by sublethal damage repair. Hence, the rationale for fractionated radiotherapy by which a consistent low dose of radiation is delivered daily allowing time for normal tissue recovery between fractions, while the cumulative dose of radiotherapy delivered to the target achieves cell kill[15]. This concept has theoretical validity, yet clinically acute toxicities often still manifest mid-way or toward the end of most radiotherapy treatment courses. A prime example is the treatment of head and neck malignancies[16]. Furthermore, chronic or late effects are common and also contribute to the morbidity of therapy. This proves that sublethal damage repair is in fact not complete with an inter-fraction interval of 24 hours. Repopulation of normal tissue following peak acute toxicity could take weeks to months. This must be considered when planning courses of radiotherapy, as both acute and late toxicities can be dose-limiting factors. Historically, late toxicities have been deemed to be more dependent on fractional dose of radiation whereas early toxicities have been proven to be sensitive to changes in the fractional dose as well as time over which radiation is delivered[15]. Despite reversibility of acute toxicity, when severe, it can lead to treatment breaks and compromise of tumor control[16]. Dose-limiting late toxicity is often irreversible, and stem from permanent radiation-induced damage of surrounding OARs. Given the above conundrums of delivering safe and effective radiotherapy, we now introduce an innovative treatment planning strategy to potentially reduce acute and late normal tissue toxicity without compromising tumor control.

In contrast to present day IMRT treatment algorithms, which deliver a consistent fractional dose of radiation to the planning target and surrounding OARs while abiding by many evidence-based constraints[2,17], we propose a novel planning technique in which the dose delivered to OARs is temporally 'feathered' to allow for improved normal tissue recovery of radiation-induced damage. In this technique, radiation dose delivered to the target of interest is assumed to remain unchanged. Reduction of normal tissue toxicity is simulated with the implementation of TFRT using a combination of the Linear-Quadratic (LQ) model to describe the immediate radiation response of normal tissue, and a mathematical model to describe normal tissue repair over time. We propose temporally feathering surrounding organs at risk while maintaining the same dose per fraction delivered to the target, and therefore will not alter or compromise tumors kill but only reduce normal tissue toxicity. The novelty is balancing normal tissue repair against damage, whereas classic radiation biologic models only account for injured tissues irrespective of time allowed for recovery our model considers these factors. The focus of this study is introducing the theoretical radiation biology behind the advance. The proposed model of NTCP with a recovery term allows for the conceptual presentation of TFRT, and development of a predictor of TFRT benefit over conventionally planned radiation therapy.

Methods

Temporally Feathered Radiotherapy

We present a novel treatment planning technique, referred to as temporally feathered radiation therapy (TFRT), in which the fractional radiation dose delivered to OARs is altered to allow for increased normal tissue recovery with respect to conventionally fractionated radiotherapy. A TFRT plan is generated as a

composite of several iso-curative (same tumor dose) plans each with altered constraints on particular OARs of interest. In each of these plans, a single OAR is deprioritized, allowing the optimization algorithm to reduce radiation dose and thereby toxicity to all other OARs. In practice, let us assume a target volume with 5 surrounding OARs of interest prescribed a dose of 70 Gy in 35 fractions, similar to that commonly implemented in treating head and neck cancers. Further, let us consider that 5 plans are developed, wherein each of the 5 OARs receives a relatively high fractional dose (d_H) compared to the standard fractional dose (d_S) once weekly, i.e. 2.0 Gy. A relatively lower (d_L) fractional dose is then delivered the remaining 4 days of the week (Figure 1). With this planning strategy, though greater sublethal damage is induced by d_H once weekly, it is offset by the lower fractional dose, d_L, delivered over a greater amount of time, i.e. during the remaining 4 days. We then compare the composite of d_H and d_L to the corresponding standard fractional dose d_S delivered to each OAR in a conventionally fractionated radiotherapy plan. In this illustrative case, the TFRT plan is composed by 35 fractions and each OAR of interest will receive 28 fractions of $d_L < d_S$ and 7 fractions of $d_H > d_S$. For demonstrative purpose, we focus analysis to a single OAR of the 5 considered, however TFRT could be applicable to any number of OARs simultaneously irrespective of the tumor site (Figure 1).

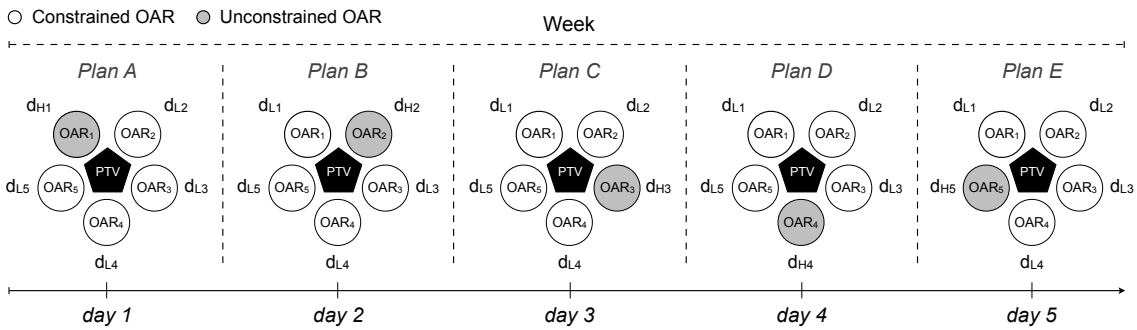

Figure 1. Schematic representation of treatment planning in temporally feathered radiation therapy (TFRT). The planning target volume (PTV) is in close proximity to 5 OARs. Each OAR *i* receives a higher fractional dose once weekly, d_{Hi}, followed by lower fractional doses for the remaining four fractions, d_{Li}, $1 \leq i \leq 5$. The PTV is represented as a black pentagon, and circles represent surrounding OARs. White: constrained OAR; Gray: unconstrained OAR.

Biologically Effective Dose (BED) Model

The current mathematical model fit to observed in vitro cell survival experiments allows modeling of surviving fraction following exposure to radiation. This model incorporates the linear-quadratic behavior of observed cell survival curves[18]. The linear component accounts for cell killing by DNA double strand breaks (DSBs) due to a single hit of radiation whereas the quadratic component represents the lethal effects of two separate ionizing events that eventually cause DSBs[15,18-19]. The surviving fraction (SF) of cells after n fractions of a radiation dose *d* is given by

$$SF(d) = e^{-nd(\alpha+\beta d)}, \tag{1}$$

where α (Gy^{-1}) and β (Gy^{-2}) are tissue-dependent radiosensitivity parameters. It follows directly from the LQ-model that the biological effect (E) of *n* equally sized fractions of dose *d* is given by $E = nd\,(\alpha + \beta d)$. This equation can be manipulated to derive biologically effective dose (BED) calculations, which is a standard quantity, which allows comparison of various fractionation schemes. BED is dependent on inherent biologic radiosensitivity of tissues, which is termed as the α to β ratio, α/β. This is also borrowed from the linear-quadratic (LQ) model[18-20]. The biologically effective dose[21] is given by

$$BED = nd\left[1 + \frac{d}{\alpha/\beta}\right]. \tag{2}$$

The BED equation above applies to conventionally fractionated radiation plans in which a same fractional dose (i.e. standard dose) is daily delivered. The BED for a standard daily fraction (BED_S) is given by

$$BED_S = n_S d_S\left[1 + \frac{d_S}{\alpha/\beta}\right] \tag{3}$$

The BED of temporally feathered plans BED_{TF} is defined as follows

$$BED_{TF} = n_L d_L \left[1 + \frac{d_L}{\alpha/\beta}\right] + n_H d_H \left[1 + \frac{d_H}{\alpha/\beta}\right], \tag{4}$$

where n_S is the number of fractions and d_S is the radiation dose per fraction delivered in a conventional fractionation. In temporally feathered plans, n_L and n_H refer to the number of lower dose fractions and number of higher dose fractions respectively. Lower dose fractions deliver a dose less than what would be delivered in a standard plan, low dose $d_L < d_S$ and similarly higher dose fractions deliver a dose higher than the fractional dose of standard plans, $d_H > d_S$. We consider that doses d_L and d_H remains unaltered during the treatment, and for this initial treatment, we consider dose to each structure to be homogeneous. Importantly, the total number of fractions and their time of delivery remains the same in conventionally fractionated and temporally feathered plans, i.e. $n_S = n_L + n_H$, and we are not changing tumor dose, only dose to OARs. The difference in the BEDs delivered by a standard plan and a temporally feathered plan is defined as $\Delta BED = BED_S - BED_{TF}$.

Dynamic NTCP Modeling

Given that temporally feathered plans allow more time for repair of normal tissue following a higher dose d_H, we use a non-spatial dynamic model to simulate normal tissue response to radiation. This is a form of normal tissue complication probability modeling (NTCP), which are quantitative measures for the expected negative side effects on healthy tissue[22-26]. The model is formulated as a logistic differential equation that describes the recovery of normal tissues (N) from sublethal radiation-induced damage given by

$$\frac{dN}{dt} = \mu\, N(t)\big(1 - N(t)\big) - \delta(t_i)\, RT(d)\, N(t)\big(1 - N(t)\big), \tag{5}$$

where the organ-specific parameter $\mu > 0$ represents the recovery rate of radiation-induced damage. We consider the case that before radiation, the OAR is at tissue homeostasis with a 1% turnover rate, $N(0) = 0.99$. Then $N(t) < N(0)$ represents the level of normal tissue damage by radiotherapy (small values of N(t) relate to severe damage), and $(N(0) - N(t))$ is used as an indication of the radiation-induced toxicity. Further, we denote by $\Delta NTCP$ as the difference between the degrees of normal tissue toxicity (radiation damage) induced by a standard $N_S(t)$ and a temporally feathered $N_{TF}(t)$ plan at the end of treatment. This means that positive values $\Delta NTCP > 0$ favor temporally feathered over conventionally fractionated plans. The logistic differential equation (5) used to model normal tissue recovery simulates a decay of toxicity to zero overtime. This is based on clinical observations revealing that not all patients develop late toxicities, and more importantly, that acute toxicities normally do go to zero on rather short time scales. Further, this model is used to compare conventionally fractionated and temporally fathered plans under the same conditions, which does not influence the ability to compare planning techniques.

The effect of radiation is included by the loss term $\delta(t_i)\, RT(d)\, N(t)\big(1 - N(t)\big)$ in Equation (5), where $\delta(t_i)$ is a characteristic function equal to 1 at the time of irradiation t_i, and zero in other case. The structure of this loss term models the growing effect of radiation therapy with increasing number of fractions. In fact, it is known that as treatment fractions accumulate the observed radiation-induced acute toxicities become increasingly apparent[27]. Clinically, we observe toxicities that increase in severity mid-way and towards the end of treatment. The function $RT(d) = \left(1 - e^{-\alpha d - \beta d^2}\right)$ is based on the radiobiological LQ model in Equation (1). More precisely, $RT(d)$ represents the "injured fraction" of normal cells receiving a radiation dose d (i.e. 1 – surviving faction of cells). Thus, for low radiation doses the injured fraction of normal cells due to radiation must be small thereby $RT(d)$ must be close to 0. On the other hand, high radiation doses will result in more killed normal cells for which $RT(d)$ tends to 1. Further, we assume that both the delivery of each fraction and response to radiation are instantaneous. It should be noted that similar models have been previously proposed to simulate the effect of radiation on brain[28] and lung tumors[29], as well as to define an organ-specific normal tissue complication probability model[30].

Results

BED Model Simulations

We first consider the BED model to compare different temporally feathered and conventionally fractionated treatments under varying conditions. Figure 2 illustrates the differences in the BED between standard and TFRT plans, defined as $\Delta BED = (BED_S - BED_{TF})$, see Equations (3) and (4). These simulations were conducted for an OAR with presumed $\alpha/\beta = 3$ Gy, and represent 35 total fractions (28 n_L with a low dose $d_L < d_S$ and 7 n_H with a high dose $d_H > d_S$ in TFRT plans). Irrespective of d_S, temporally feathered plans result only in a lower BED when the total dose delivered to the OAR (28 d_L + 7 d_H) is less compared to the standard plan (35 d_S). Further, combinations of d_L and d_H exist in which $BED_{TF} > BED_S$ even when the total dose by TFRT plans is smaller than in the standard plan. These results hold irrespective of the α/β ratio of the OAR of interest (see Supplementary Figure 1). Thus, due to the fact that the BED formulation does not consider the effect of inter-fractional normal tissue repair of radiation-induced damage, this is not a suitable model to evaluate the potential benefit of temporal feathering with respect to conventionally fractionated radiotherapy. Indeed, this highlights the need for models considering the dynamic of tissue repair between treatment fractions to assess the success potential of TFRT.

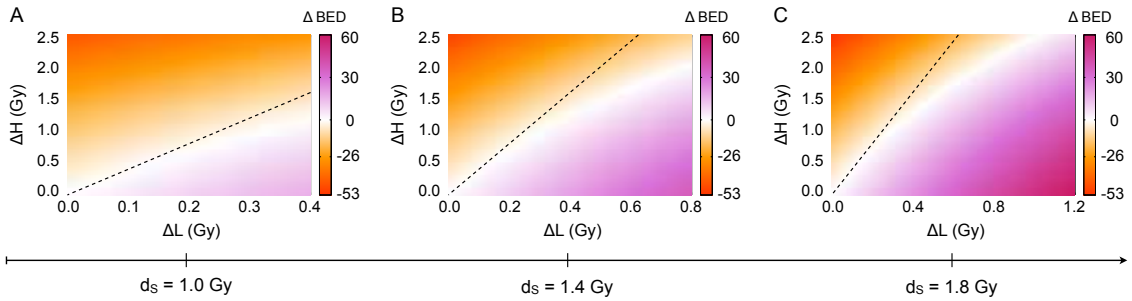

Figure 2. Comparison of conventionally fractionated and temporally feathered radiation therapy based on the biologically effective dose (BED) model. $\Delta BED = (BED_S - BED_{TF})$ is defined as the difference in the BEDs delivered by a standard plan and a temporally feathered plan. **(A-C)** From left to right representation of ΔBED delivered to an OAR with $\alpha/\beta = 3$ Gy by standard plans of d_S in 35 fractions and TFRT plans with $n_L = 28$ and $n_H = 7$. The x- and y-axes represent $\Delta L = d_S - d_L$ and $\Delta H = d_H - d_S$ respectively. Combinations of d_L and d_H remain unaltered during the course of treatments. The dashed line shows the plot at which the total dose of temporally feathered and standard plans are equal ($\Delta H = 4\ \Delta L$). The region below (above) the dashed line represents combinations of d_L and d_H in which TFRT plans deliver lower (higher) total doses compared to a standard plan, keeping d_S constant.

Dynamic NTCP Model Simulations

We now simulate normal tissue complication probability (NTCP) of TFRT compared to conventionally fractionated radiation therapy by means of the model of normal tissue response and recovery in Equation (5). In this model, the organ-dependent recovery rate is represented by μ (day^{-1}), and radiation effect on normal cells described by the LQ model in Equation (1). Proof of principle exists in the particular case investigated as follows. We consider a conventionally fractionated plan delivering d_S in 35 fractions, and TFRT plans consisting of 28 fractions (n_L) of $d_L < d_S$ and 7 fractions (n_H) of $d_H > d_S$. Further, we assume an OAR of interest at a physiologic equilibrium and characterized by a α/β ratio of 3 Gy (model simulations for varying α/β ratios are available in the Supplementary Material).

Simulations conducted using the NTCP model in Equation (5) reveal a range of conditions in which TFRT plans reduce radiation-induced toxicity to OARs compared to conventionally fractionated plans. These conditions are dependent on d_L and d_H, as well as on the organ-specific recovery rates μ, associated with radiation damage. This is shown in Figures 3 and 4, which illustrate the differences between conventionally fractionated and temporally feathered plans (ΔNTCP) with varying values of the recovery rate μ. For each μ value, the bottom panels represent ΔNTCP resulting from a standard plan with a constant daily dose d_S, and combinations of d_L and d_H in TFRT plans varying in the ranges $[d_S - 0.5, d_S]$ and $[d_S, d_S + 2.5]$ respectively. We found that certain combinations of d_L and d_H may deliver higher total doses in TFRT

plans as compared to standard plans (28 d_L + 7 d_H > 35 d_S) but yet still reduce the overall OAR toxicity at the end of treatment. This is depicted by the region above the dashed line (red: ΔNTCP > 0) in the bottom panels of Figure 3. This particular scenario emphasizes the opportunity of reducing OAR toxicity using TFRT despite increased total dose delivered to the OAR of interest, and also suggests technical feasibility.

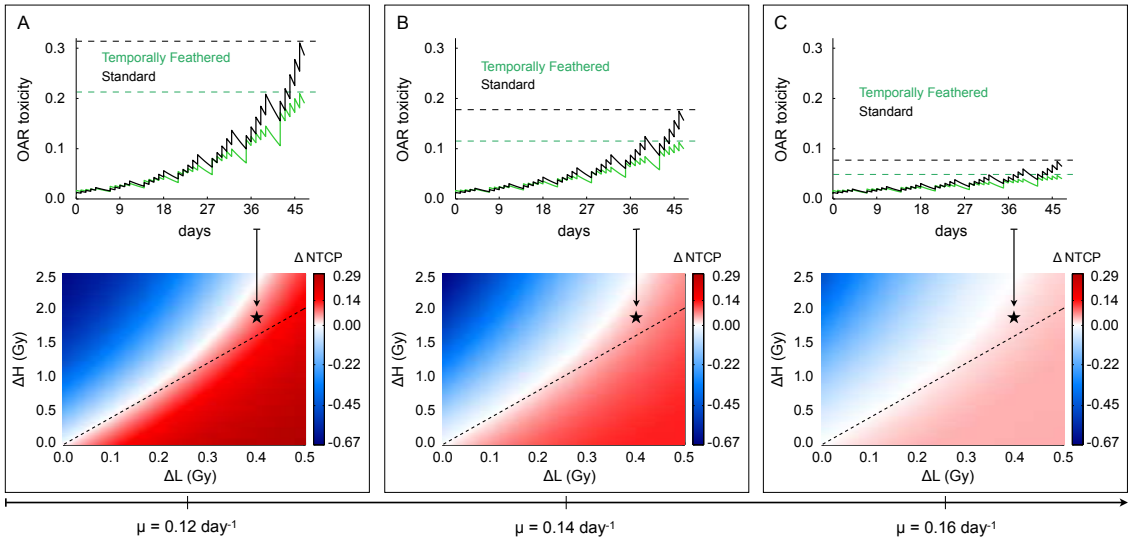

Figure 3. Comparison and representation of NTCP and OAR toxicity of conventionally fractionated and TFRT plans with varying recovery rates (μ). NTCP modeling follows Equation (5) and is simulated for an OAR with α/β = 3 Gy. The x- and y-axes represent $\Delta L = d_S - d_L$ and $\Delta H = d_H - d_S$ respectively. Combinations of doses d_L and d_H remain unaltered during the course of treatments. **(A-C)** Bottom panels from left to right ΔNTCP are obtained for increasing OAR recovery rates (μ), under conditions of d_S = 1.2 Gy in 35 fractions, n_L = 28 and n_H = 7. The dashed line shows the plot at which the total dose of temporally feathered and standard plans are equal. The region below (above) the dashed line represents combinations of d_L and d_H in which TFRT plans deliver lower (higher) total doses compared to a standard plan, keeping d_S constant. Top sub-figures show the time-evolution of OAR toxicity induced by the standard (black) and TFRT (green) plans corresponding to the location marked by stars in bottom panels. Dashed lines represent the time points at which NTCP of standard and TFRT plans are compared.

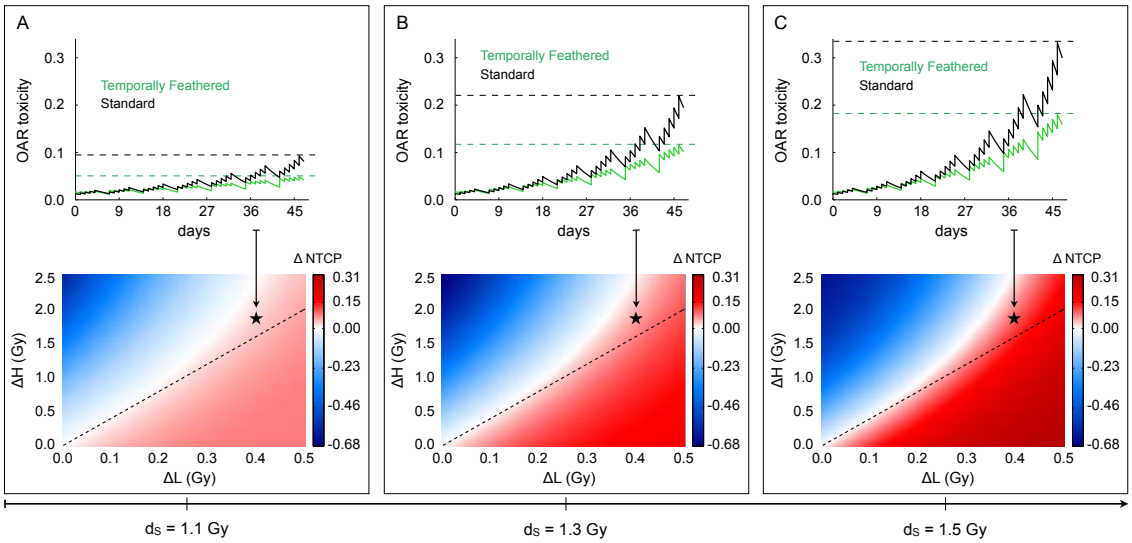

Figure 4. Comparison and representation of NTCP and OAR toxicity of conventionally fractionated and TFRT plans with varying standard fractional dose (d_S). NTCP modeling follows equation (5) and is simulated for OAR late toxicity (α/β = 3 Gy). The x- and y-axes represent $\Delta L = d_S - d_L$ and $\Delta H = d_H - d_S$ respectively. Combinations of doses d_L and d_H remain unaltered during the course of treatments. **(A-C)** Bottom panels from left to right ΔNTCP are obtained for increasing standard fractional doses d_S in 35 fractions, under conditions of μ = 0.15 day^{-1}, n_L = 28 and n_H = 7. Top sub-figures show the time-evolution of OAR toxicity induced by the standard (black) and temporally feathered

(green) plans corresponding to the location marked by stars in bottom panels. Dashed lines represent the time points at which NTCP of conventionally fractionated and TFRT plans are compared.

Another important finding is that the therapeutic gain by TFRT increases as the treatment progresses. This is shown in the top plots of Figures 3 and 4, where, irrespective of the values of μ and standard doses d_S considered, the difference in the radiation induced damage by conventionally fractionated and TFRT plans progressively increases with the number of treatment fractions. Figure 3 illustrates the utility of TFRT in reducing toxicity in OARs with low recovery rates (μ) when compared to standard plans delivering d_S = 1.2Gy per fraction. Furthermore, reduction in OAR toxicity by TFRT plans is greater when compared to standard fractionation protocols delivering higher doses d_S to the OAR of interest with μ = 0.15 day^{-1}, as shown in Figure 4. However, previous results strongly depend on the particular combination of μ and d_S where a close relationship exists. More precisely, optimal success potentials and maximum benefit can be achieved with TFRT as d_S or μ values change. While keeping constant any of those parameters and varying the other, we found that the potential benefit of TFRT increases until a maximum level and then decreases again (Figure 4).

To better assess the performance of TFRT as a method of normal tissue toxicity reduction, Figure 5 summarizes how organ-specific and treatment parameters impact the success potential of TFRT. For each combination of μ and d_S, ΔNTCP of the standard plan delivering d_S and the TFRT plan with $(d_S - 0.5) \leq d_L \leq d_S$ and $d_S \leq d_H \leq (d_S + 2.5)$ are provided. Figure 5(A) summarizes the overall potential benefit of TFRT plans compared to conventionally fractionated radiotherapy, referred to as OPB_{TF}, and obtained as the ratio of temporally feathered plans resulting in (ΔNTCP > 0) and delivering higher total doses ($28\ d_L + 7\ d_H > 35\ d_S$) than the corresponding standard plan to all simulated treatment plans. Further, the maximum potential benefit of TFRT plans, referred to as MAX_{TF}, is shown in Figure 5(B). MAX_{TF} is obtained as the maximum ΔNTCP > 0 of TFRT plans delivering higher total doses than the corresponding standard plan.

Considering the entire parameter space reveals the limits of TFRT benefit, and also gives us an opportunity to use retrospective data to parameterize individual OAR recovery rates (μ), and to appropriate select patients in the future. We leave this to future work however. Supplementary Figures 2 and 3 show that overall potential benefit (OPB_{TF}) and maximum potential benefit (MAX_{TF}) of TFRT plans also depend on the specific α/β ratio of the OAR of interest. However, TFRT continues to be a possible, valuable alternative to reduce radiation induced OAR damage.

Discussion

The rationale of radiation therapy is maximizing the therapeutic ratio such that tumor control is balanced against induced normal tissue toxicity. Through the years, researchers in the field of radiation oncology and medical physics have been innovating new ways of widening the therapeutic ratio by either increasing tumor control probability (TCP) or decreasing normal tissue complication probability (NTCP). In this study, we focus on the latter. We introduce TFRT as a new treatment planning strategy that alters fractional doses of radiation delivered to OARs over time to maximize normal tissue recovery through the course of treatment. TFRT planning capitalizes on the non-linearity of normal tissue recovery, allowing non-intuitively for more sublethal damage repair and repopulation even in the face of higher total dose delivered at the en of treatment. For this purpose, we used the Linear-Quadratic (LQ) model to describe the immediate radiation response of normal tissue and a dynamical NTCP model to describe normal tissue repair over time.

We notice that similar models have been previously proposed to simulate the effect of radiation on brain[28] and lung tumors[29], as well as to define an organ specific normal tissue complication probability model[30]. The proposed model of NTCP is pivotal to the demonstration of improved normal tissue recovery with altered fractionation schemes, since the well-accepted standard LQ model is limited by the lack of a recovery term. Further, the model considered is sensitive to parameter changes including recovery rate (μ), α/β ratio and standard fractional dose d_S. This is a strength of the model as these parameters represent phenomenological values, which make this model personalizable to different clinical scenarios. Recently, work on Genomic Radiation Dosing has shown the wide heterogeneity response to radiation therapy[14]. The

α/β ratio and μ are organ-specific parameters, and will therefore determine the potential of TFRT to reduce toxicity of each organ involved. This aids in assigning priorities to the OARs for optimization based on the therapeutic gain of TFRT. Then, the fractional dose could be determined by an optimization method that considers the specific organs involved. We have provided additional simulation changes in TFRT plan outcomes depending on model parameters in the Supplementary Material. Thus, model sensitivity to parameter changes is just highlighting that the potential of TFRT depends on the specific organs involved on each clinical case, and opportunities for personalization once we better understand this first step.

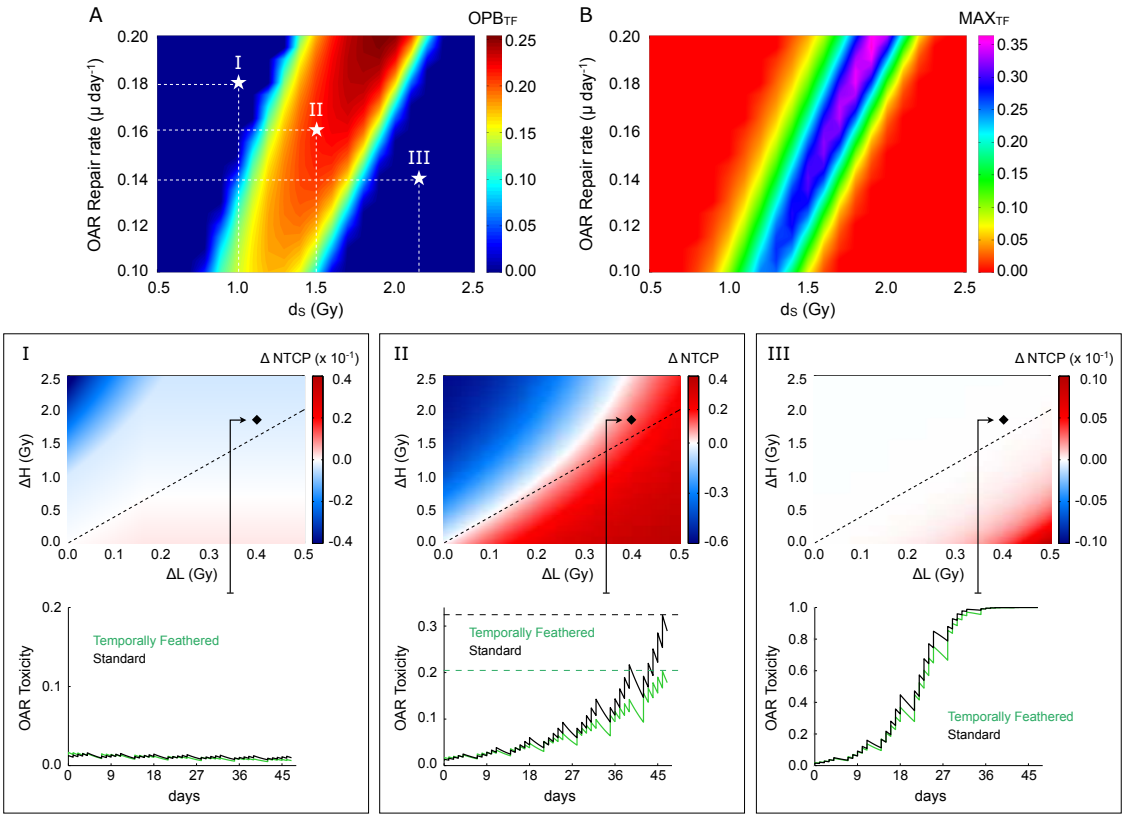

Figure 5. Overall potential benefit of TFRT plans over conventionally fractionated radiation therapy with respect to the standard fractional dose (d_S) and OAR damage repair rate (μ). For each combination of μ and d_S, ΔNTCP values are obtained for an OAR with α/β = 3 Gy as a result of comparing a standard plan delivering d_S in 35 fractions and TFRT plans consisting in 28 fractions of $(d_S - 0.5) \leq d_L \leq d_S$ and 7 fractions of $d_S \leq d_H \leq (d_S + 2.5)$. Combinations of doses d_L and d_H remain unaltered during the course of treatments. **(A)** Overall potential benefit (OPB_{TF}) is defined as the ratio of TFRT plans resulting in ΔNTCP > 0 and delivering higher total doses than the corresponding standard plan to all simulated plans. **(B)** Maximum potential benefit (MAX_{TF}) achieved with TFRT plans resulting in ΔNTCP > 0 and delivering higher total doses than the corresponding standard plan. Top panels in **I**, **II** and **III** represent the single cases marked by stars in (A). The x- and y-axes represent $\Delta L = d_S - d_L$ and $\Delta H = d_H - d_S$ respectively. Bottom panels in **I**, **II** and **III** show time-evolution of OAR toxicity induced by the standard (black) and TFRT (green) plans corresponding to the location marked by diamonds in the top panels.

Feasibility of TFRT was evaluated by considering different combinations of model parameters d_S and μ as described above. We have provided "overall potential benefit" maps to help gauge the potential of TFRT plans in reducing normal tissue toxicity as compared to conventionally fractionated plans (see Figure 5, and Supplementary Figures 2 and 3). Overall potential benefit of TFRT is dependent on recovery rates and radiation doses per fraction delivered to OARs of interest. It should be noted that TFRT has the most potential to reduce OAR toxicity in carefully selected patients whereas the gain might not be substantial for all comers treated with IMRT. The ideal patient is likely to be one where traditionally achieved doses to OARs are near their tolerance and recovery rates are average to low. Regardless of the inherent radiosensitivity of the normal tissue (i.e. α/β ratio), TFRT plans can be a superior treatment choice (see Supplementary Figures 2 and 3). Though this analysis lacks clinical data, the NTCP model is compelling and warrants further evaluation. Future work will be focused on studying individual patient-specific

dosimetric plans comparing standard IMRT versus TFRT, for instance with respect to dose-volume histogram (DVH) based metrics with clinical relevance[31]. To allow application in the clinic, there is need to create an optimized workflow. An automated planning algorithm will be generated with input factors for dose and fractionation delivered to OAR and recovery rates (μ) for OARs of interest. Efforts will need to be directed toward elucidating recovery rates of normal tissues. Based on radiobiological properties of the OARs involved, the introduced TFRT technique has the potential to inform about the optimal sparing frequency and combinations of OARs to be considered for each daily treatment plan, as well as how many plans are required for individual radiotherapy patients. These models can be fit to clinical toxicity data to create a definition of the OAR radiation damage recovery rate (μ). Moreover, the concept of TFRT can be applied to any site, and it is most useful in cases in which the target lies within close proximity to multiple surrounding organs at risk.

The impact of these new techniques is reduction of OAR toxicity to *(i)* improve quality of life issues for patients experiencing both acute and late complications of radiation-induced toxicity, and *(ii)* enable dose escalation to the tumor for patients currently failing radiation. The next step beyond TFRT is its combination with spatial information. As focus has been redirected away from looking at organs in their entirety and instead more so as partial volumes with evolving dose constraints, gradients of dose across the normal tissue of interest have been emphasized[32]. We hope to use data points beyond simple dose volume histogram data in predicting the risk of toxicity since these do not take into consideration spatial, anatomic, or biologic effects of where dose is actually distributed. Dividing OAR into sub-volumes may better estimate and characterize the toxicity induced by each treatment plan.

Conclusions

We introduce a novel strategy of radiation treatment planning termed temporally feathered radiation therapy (TFRT), in which the fractional dose delivered to each organ at risk (OAR) is varied allowing increased time for normal tissue recovery. TFRT plans deliver to the OARs a higher dose once weekly followed by four lower fractional doses. Normal tissue toxicity induced by TFRT and conventional fractionated plans is compared by using a combination of the Linear-Quadratic (LQ) model to describe the immediate radiation response, and a NTCP model to describe normal tissue repair over time. The proposed NTCP model of temporally feathering OARs demonstrates less toxicity despite higher total doses of radiation delivered with TFRT compared to conventionally fractionated plans. Clinically, reduced OAR toxicity contributes to increased patient quality of life while undergoing radiation therapy, upon completion of treatment, and overall less treatment breaks. Furthermore, isotoxic radiation doses can be delivered as an avenue for dose escalation to the planning target. These results are compelling and warrant further evaluation in the clinical setting.

Acknowledgements

J. C. L. Alfonso gratefully acknowledges the funding support of the German Federal Ministry of Education and Research (BMBF) for the eMED project SYSIMIT (01ZX1308D). J. G. Scott thanks the NIH Loan repayment program for their generous support of his research. This research is partially supported by the Andrew Sabin Family Foundation; Dr. Fuller is a Sabin Family Foundation Fellow. Dr. Fuller receives direct funding and salary support from the National Institutes of Health (NIH), including: the National Institute for Dental and Craniofacial Research Award (1R01DE025248-01/R56DE025248-01); a National Science Foundation (NSF), Division of Mathematical Sciences, Joint NIH/NSF Initiative on Quantitative Approaches to Biomedical Big Data (QuBBD) Grant (NSF 1557679); the NIH Big Data to Knowledge (BD2K) Program of the National Cancer Institute (NCI) Early Stage Development of Technologies in Biomedical Computing, Informatics, and Big Data Science Award (1R01CA214825-01); NCI Early Phase Clinical Trials in Imaging and Image-Guided Interventions Program (1R01CA218148-01); an NIH/NCI Cancer Center Support Grant (CCSG) Pilot Research Program Award from the UT MD Anderson CCSG Radiation Oncology and Cancer Imaging Program (P30CA016672) and an NIH/NCI Head and Neck Specialized Programs of Research Excellence (SPORE) Developmental Research Program Award (P50 CA097007-10). Dr. Fuller receives salary support from the Patient-Centered Outcomes Research Institute (PCORI). Dr. Fuller has received direct industry grant support and travel funding from Elekta AB.

Supplementary Material

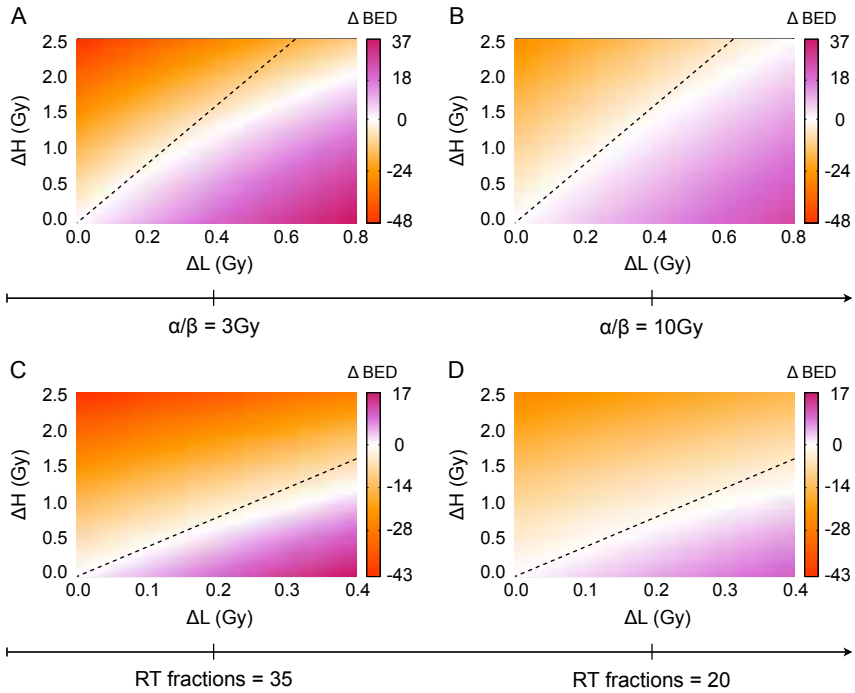

Supplementary Figure 1: Comparison of conventionally fractionated and temporally feathered radiation therapy based on the biologically effective dose (BED) model. $\Delta BED = (BED_S - BED_{TF})$ is defined as the difference in the BEDs delivered by a standard plan and a temporally feathered plan. **(A,B)** Representation of ΔBED delivered to OARs with different α/β ratios by a standard plan of d_S = 1.4Gy in 35 fractions and TFRT plans consisting in 28 fractions of $d_L < d_S$ and 7 fractions of $d_H > d_S$. **(C)** Representation of ΔBED delivered to an OAR with α/β = 3Gy by a standard plan of d_S = 1.0Gy in 20 fractions and TFRT plans consisting in 16 fractions of $d_L < d_S$ and 4 fractions of $d_H > d_S$. **(D)** Representation of ΔBED delivered to an OAR with α/β = 3Gy by a standard plan of d_S = 1.0Gy in 35 fractions and TFRT plans consisting in 28 fractions of $d_L < d_S$ and 7 fractions of $d_H > d_S$. The x- and y-axes represent $\Delta L = d_S - d_L$ and $\Delta H = d_H - d_S$ respectively. Combinations of d_L and d_H remain unaltered during the course of treatments. The dashed line shows the plot at which the total dose of temporally feathered and conventional plans are equal (ΔH = 4 ΔL). The region below (above) the dashed line represents combinations of d_L and d_H in which TFRT plans deliver lower (higher) total doses compared to a conventional plan, keeping d_S constant.

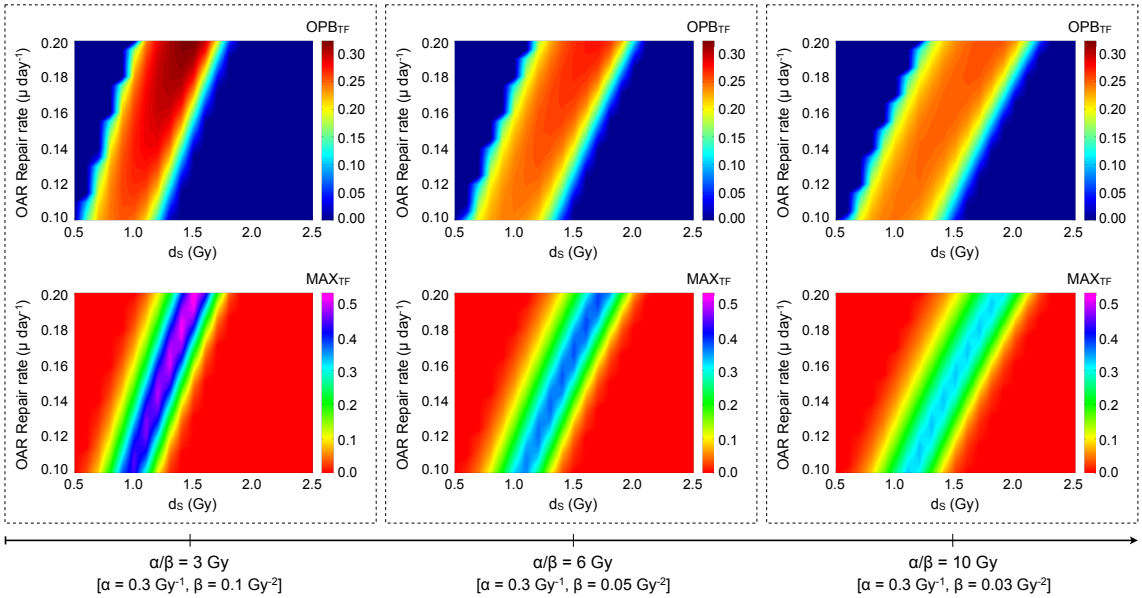

Supplementary Figure 2: Overall potential benefit of TFRT plans over conventionally fractionated radiation therapy, for OARs with different α/β ratios obtained by varying β, with respect to the standard fractional dose (d_S) and OAR damage repair rate (μ). For each combination of μ and d_S, ΔNTCP values are obtained as a result of comparing a standard plan delivering d_S in 35 fractions and TFRT plans consisting in 28 fractions of $(d_S - 0.5) \leq d_L \leq d_S$ and 7 fractions of $d_S \leq d_H \leq (d_S + 2.5)$. **Top panels:** overall potential benefit (OPB_{TF}) is defined as the ratio of TFRT plans resulting in ΔNTCP > 0 and delivering higher total doses than the corresponding standard plan to all simulated plans. **Bottom panels:** maximum potential benefit (MAX_{TF}) achieved with TFRT plans resulting in ΔNTCP > 0 and delivering higher total doses than the corresponding standard plan.

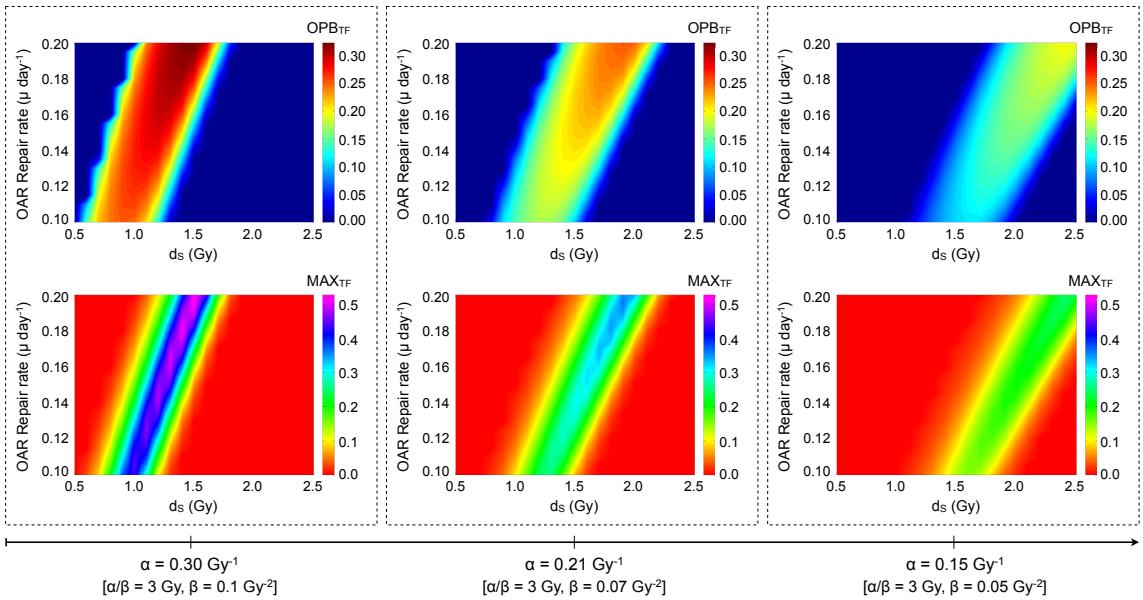

Supplementary Figure 3: Overall potential benefit of TFRT plans over conventionally fractionated radiation therapy, for an OAR with α/β = 3 Gy obtained by varying α and β, with respect to the standard fractional dose (d_S) and OAR damage repair rate (μ). For each combination of μ and d_S, ΔNTCP values are obtained as a result of comparing a standard plan delivering d_S in 35 fractions and TFRT plans consisting in 28 fractions of $(d_S - 0.5) \leq d_L \leq d_S$ and 7 fractions of $d_S \leq d_H \leq (d_S + 2.5)$. **Top panels:** overall potential benefit (OPB_{TF}) is defined as the ratio of TFRT plans resulting in ΔNTCP > 0 and delivering higher total doses than the corresponding standard plan to all simulated plans. **Bottom panels:** maximum potential benefit (MAX_{TF}) achieved with TFRT plans resulting in ΔNTCP > 0 and delivering higher total doses than the corresponding standard plan.

References

1- Atun R, Jaffray DA, Barton MB, et al. Expanding global access to radiotherapy. Lancet Oncol. 16(10): 1153–86, 2015. doi: 10.1016/S1470-2045(15)00222-3.

2- Emami B, Lyman J, Brown A, et al. Tolerance of normal tissue to therapeutic irradiation. Int J Radiat Oncol Biol Phys. 21(1): 109–22, 1991. doi: http://dx.doi.org/10.1016/0360-3016(91)90171-Y.

3- Purdy JA. Dose to normal tissues outside the radiation therapy patient's treated volume: a review of different radiation therapy techniques. Health Phys. 95(5): 666-76, 2008. doi: 10.1097/01.HP.0000326342.47348.06.

4- Bortfeld T, Bürkelbach J, Boesecke R, Schlegel W. Methods of image reconstruction from projections applied to conformation radiotherapy. Phys Med Biol. 35(10): 1423-34, 1990. doi: https://doi.org/10.1088/0031-9155/35/10/007.

5- Brahme A. Optimization of stationary and moving beam radiation therapy techniques. Radiother Oncol. 12(2): 129-40, 1988. doi: https://doi.org/10.1016/0167-8140(88)90167-3.

6- Bortfeld TR, Kahler DL, Waldron TJ, Boyer AL. X-ray field compensation with multileaf collimators. Int J Radiat Oncol Biol Phys. 28(3): 723-30, 1994. doi: https://doi.org/10.1016/0360-3016(94)90200-3.

7- Scott JG, Fletcher AG, Anderson AR, Maini PK. Spatial metrics of tumour vascular organisation predict radiation efficacy in a computational model. PLoS Comput Biol. 12(1): e1004712, 2016. doi: 10.1371/journal.pcbi.1004712.

8- Citrin D, Cotrim AP, Hyodo F, Baum BJ, Krishna MC, Mitchell JB. Radioprotectors and mitigators of radiation-induced normal tissue injury. Oncologist. 15(4): 360-71, 2010. doi: 10.1634/theoncologist.2009-S104.

9- Wardman P. Chemical radiosensitizers for use in radiotherapy. Clin Oncol. 19(6): 397-417, 2007. doi: https://doi.org/10.1016/j.clon.2007.03.010.

10- Fu KK, Pajak TF, Trotti A, et al. A Radiation Therapy Oncology Group (RTOG) phase III randomized study to compare hyperfractionation and two variants of accelerated fractionation to standard fractionation radiotherapy for head and neck squamous cell carcinomas: first report of RTOG 9003. Int J Radiat Oncol Biol Phys. 48(1): 7-16, 2000. doi: http://dx.doi.org/10.1016/S0360-3016(00)00663-5.

11- Chang BK, Timmerman RD. Stereotactic body radiation therapy: a comprehensive review. Am J Clin Oncol. 30(6): 637-44, 2007. doi: 10.1097/COC.0b013e3180ca7cb1.

12- Ahmed KA, Correa CR, Dilling TJ, et al. Altered fractionation schedules in radiation treatment: a review. Semin Oncol. 41(6): 730-50, 2014. doi: 10.1053/j.seminoncol.2014.09.012.

13- Unkelbach J, Papp D. The emergence of nonuniform spatiotemporal fractionation schemes within the standard BED model. Med Phys. 42(5): 2234-41, 2015. doi: 10.1118/1.4916684.

14- Scott JG, Berglund A, Schell MJ, et al. A genome-based model for adjusting radiotherapy dose (GARD): a retrospective, cohort-based study. Lancet Oncol. 18(2): 202-11, 2017. doi: 10.1016/S1470-2045(16)30648-9.

15- Hall EJ, Giaccia, AJ. Radiobiology for the Radiologist. Lippincott Williams & Wilkins, 2006.

16- Dirix P, Nuyts S. Evidence-based organ-sparing radiotherapy in head and neck cancer. Lancet Oncol. 11(1): 85-91, 2010. doi: 10.1016/S1470-2045(09)70231-1.

17- Bentzen SM, Constine LS, Deasy JO, et al. Quantitative Analyses of Normal Tissue Effects in the Clinic (QUANTEC): an introduction to the scientific issues. Int J Radiat Oncol Biol Phys. 76(3 Suppl): S3-9, 2010. doi: 10.1016/j.ijrobp.2009.09.040.

18- Brenner DJ. The linear-quadratic model is an appropriate methodology for determining isoeffective doses at large doses per fraction. Semin Radiat Oncol. 18(4): 234-9, 2008. doi: 10.1016/j.semradonc.2008.04.004.

19- Fowler JF. The linear-quadratic formula and progress in fractionated radiotherapy. Br J Radiol. 62(740): 679-94, 1989. doi: https://doi.org/10.1259/0007-1285-62-740-679.

20- Jones B, Dale RG, Deehan C, Hopkins KI, Morgan DA. The role of biologically effective dose (BED) in clinical oncology. Clin Oncol. 13(2): 71-81, 2001. doi: http://dx.doi.org/10.1053/clon.2001.9221.

21- Fowler JF, Welsh JS, Howard SP. Loss of biological effect in prolonged fraction delivery. Int J Radiat Oncol Biol Phys. 59(1): 242-9, 2004. doi: http://dx.doi.org/10.1016/j.ijrobp.2004.01.004.

22- Lyman JT. Complication probability as assessed from dose-volume histograms. Radiat Res Suppl. 8(104): S13-9, 1985. doi: 10.2307/3583506.

23- Marks LB, Yorke ED, Jackson A, et al. Use of normal tissue complication probability models in the clinic. Int J Radiat Oncol Biol Phys. 76(3 Suppl):S10-9, 2010. doi: 10.1016/j.ijrobp.2009.07.1754.

24- Niemierko A, Goitein M. Modeling of normal tissue response to radiation: the critical volume model. Int J Radiat Oncol Biol Phys. 25(1): 135-45, 1993. doi: https://doi.org/10.1016/0360-3016(93)90156-P.

25- Stavrev P, Stavreva N, Niemierko A, Goitein M. Generalization of a model of tissue response to radiation based on the idea of functional subunits and binomial statistics. Phys Med Biol. 46(5): 1501-18, 2001. doi: https://doi.org/10.1088/0031-9155/46/5/312.

26- Hanin L, Zaider M. A mechanistic description of radiation-induced damage to normal tissue and its healing kinetics. Phys Med Biol. 58(4): 825-39, 2013. doi: 10.1088/0031-9155/58/4/825.

27- Eisbruch A, Harris J, Garden AS, et al. Multi-institutional trial of accelerated hypofractionated intensity-modulated radiation therapy for early-stage oropharyngeal cancer (RTOG 00-22). Int J Radiat Oncol Biol Phys. 76(5): 1333-8, 2010. doi: 10.1016/j.ijrobp.2009.04.011.

28- Rockne R, Rockhill JK, Mrugala M, et al. Predicting the efficacy of radiotherapy in individual glioblastoma patients in vivo: a mathematical modeling approach. Phys Med Biol. 55(12): 3271-85, 2010. doi: 10.1088/0031-9155/55/12/001.

29- Prokopiou S, Moros EG, Poleszczuk J, et al. A proliferation saturation index to predict radiation response and personalize radiotherapy fractionation. Radiat Oncol. 10:159, 2015. doi: 10.1186/s13014-015-0465-x.

30- Stocks T, Hillen T, Gong J, Burger M. A stochastic model for the normal tissue complication probability (NTCP) and applications. Math Med Biol. 34(4): 469-92, 2017. doi: 10.1093/imammb/dqw013.

31- Alfonso JCL, Herrero MA, Núñez L. A dose-volume histogram based decision-support system for dosimetric comparison of radiotherapy treatment plans. Radiat Oncol. 10(1): 263, 2015.
doi: 10.1186/s13014-015-0569-3.

32- van Luijk P, Pringle S, Deasy JO, et al. Sparing the region of the salivary gland containing stem cells preserves saliva production after radiotherapy for head and neck cancer. Sci Transl Med. 7(305): 305ra147, 2015. doi: 10.1126/scitranslmed.aac4441.